SOI: 1.1/TAS DOI: 10.15863/TAS

International Scientific Journal
Theoretical & Applied Science

p-ISSN: 2308-4944 (print) **e-ISSN:** 2409-0085 (online)

Year: 2023 **Issue:** 01 **Volume:** 117

Published: 24.01.2023 **http://T-Science.org**

Issue Article

Denis Chemezov
Vladimir Industrial College
M.Sc.Eng., Corresponding Member of International Academy of Theoretical and Applied Sciences, Lecturer, Russian Federation
https://orcid.org/0000-0002-2747-552X
vic-science@yandex.ru

Semyon Galaktionov
Vladimir Industrial College
Student, Russian Federation

Viktoriya Korolyova
Vladimir Industrial College
Student, Russian Federation

Ilya Prokhorov
Vladimir Industrial College
Student, Russian Federation

Vladislav Gonchar
Vladimir Industrial College
Student, Russian Federation

Egor Prozorov
Vladimir Industrial College
Student, Russian Federation

Mikhail Chebotaryov
Vladimir Industrial College
Student, Russian Federation

REFERENCE DATA OF PRESSURE DISTRIBUTION ON THE SURFACES OF AIRFOILS HAVING THE NAMES BEGINNING WITH THE LETTER O

Abstract: *The results of the computer calculation of air flow around the airfoils having the names beginning with the letter O are presented in the article. The contours of pressure distribution on the surfaces of the airfoils at angles of attack of 0, 15 and -15 degrees in conditions of the subsonic airplane flight speed were obtained.*

Key words: *airfoil, angle of attack, pressure, surface.*

Language: *English*

Citation: Chemezov, D., et al. (2023). Reference data of pressure distribution on the surfaces of airfoils having the names beginning with the letter O. *ISJ Theoretical & Applied Science, 01 (117)*, 624-635.

Soi: http://s-o-i.org/1.1/TAS-01-117-50 ***Doi***: crossref https://dx.doi.org/10.15863/TAS.2023.01.117.50

Scopus ASCC: *1507.*

Introduction

Creating reference materials that determine the most accurate pressure distribution on the airfoil surfaces is an actual task of the airplane aerodynamics.

Materials and methods

The study of air flow around the airfoils was carried out in a two-dimensional formulation by means of the computer calculation in the *Comsol Multiphysics* program. The airfoils in the cross section were taken as objects of research [1-31]. In this work, the airfoils having the names beginning with the letter *O* were adopted. Air flow around the airfoils was carried out at angles of attack (α) of 0, 15 and -15 degrees. Flight speed of the airplane in each case was subsonic. The airplane flight in the atmosphere was carried out under normal weather conditions. The geometric characteristics of the studied airfoils are presented in the Table 1. The geometric shapes of the airfoils in the cross section are presented in the Table 2.

Table 1. The geometric characteristics of the airfoils.

Airfoil name	Max. thickness	Max. camber	Leading edge radius	Trailing edge thickness
OAF095	9.48% at 23.2% of the chord	3.79% at 53.1% of the chord	1.1073%	0.5153%
OAF102	10.17% at 28.7% of the chord	3.63% at 53.1% of the chord	0.9518%	1.0018%
OAF117	11.47% at 23.2% of the chord	2.03% at 46.9% of the chord	1.6813%	0.9973%
OAF128	12.79% at 23.2% of the chord	0.99% at 43.7% of the chord	2.2047%	1.0653%
OAF139	13.67% at 23.2% of the chord	0.03% at 0.1% of the chord	2.1665%	0.9757%
ONERA NACA CAMBRE	11.52% at 31.0% of the chord	1.38% at 15.7% of the chord	1.3411%	0.24%
ONERA OA206	6.01% at 31.8% of the chord	0.84% at 19.6% of the chord	0.4632%	0.3348%
ONERA OA209	9.01% at 29.3% of the chord	1.56% at 17.1% of the chord	1.154%	0.5023%
ONERA OA212	12.01% at 31.8% of the chord	2.29% at 31.8% of the chord	2.0675%	0.67%
ONERA OA213	12.57% at 32.5% of the chord	3.32% at 25.0% of the chord	1.2962%	0.4216%
ONERA/Aerospatiale OAF095	9.48% at 23.2% of the chord	3.79% at 53.1% of the chord	1.1063%	0.515%
ONERA/Aerospatiale OAF102	10.17% at 28.7% of the chord	3.63% at 53.1% of the chord	0.9514%	1.002%
ONERA/Aerospatiale OAF117	11.47% at 23.2% of the chord	2.03% at 46.9% of the chord	1.6805%	0.997%
ONERA/Aerospatiale OAF128	12.79% at 23.2% of the chord	0.99% at 43.7% of the chord	2.2024%	1.065%
ONERA/Aerospatiale OAF139	13.67% at 23.2% of the chord	0.03% at 0.1% of the chord	2.1638%	0.976%
Ornithopter airfoil,	15.08% at 35.0% of the chord	5.04% at 50.9% of the chord	1.1514%	0.0%

Note:
ONERA/Aerospatiale OAF095, ONERA/Aerospatiale OAF102, ONERA/Aerospatiale OAF117, ONERA/Aerospatiale OAF128, ONERA/Aerospatiale OAF139 (Fenestron airfoil).

Table 2. The geometric shapes of the airfoils in the cross section.

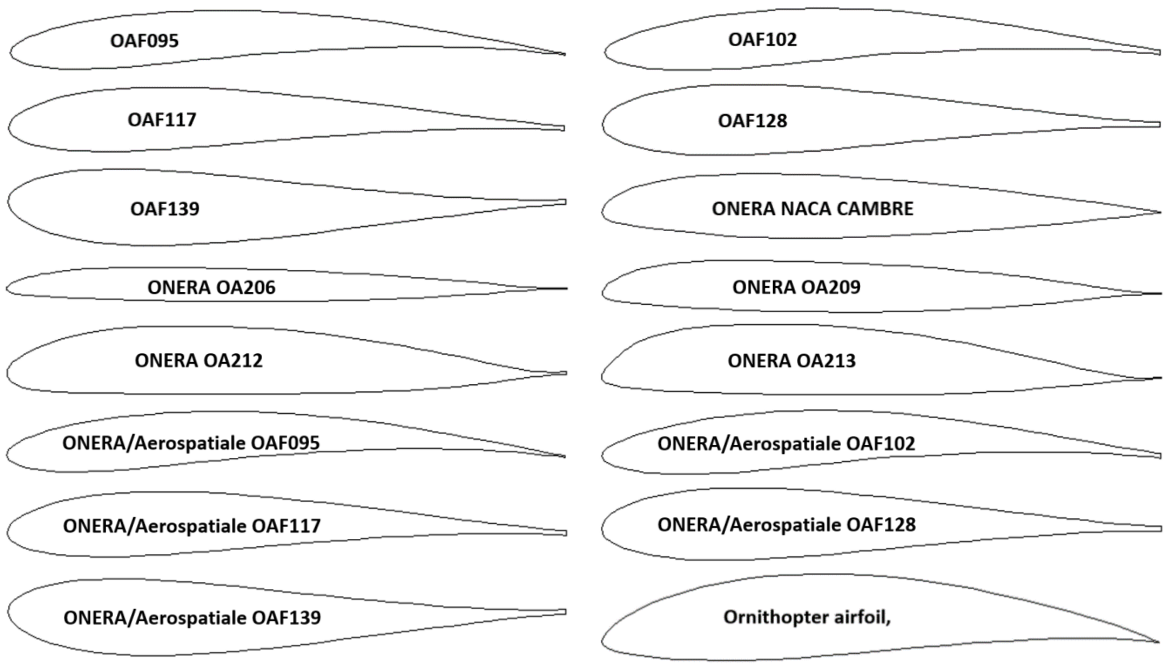

Impact Factor:	ISRA (India) = 6.317	SIS (USA) = 0.912	ICV (Poland) = 6.630
	ISI (Dubai, UAE) = 1.582	РИНЦ (Russia) = 3.939	PIF (India) = 1.940
	GIF (Australia) = 0.564	ESJI (KZ) = 8.771	IBI (India) = 4.260
	JIF = 1.500	SJIF (Morocco) = 7.184	OAJI (USA) = 0.350

Results and discussion

The calculated pressure contours on the surfaces of the airfoils at different angles of attack are presented in the Figs. 1-16. The calculated values on the scale can be represented as the basic values when comparing the pressure drop under conditions of changing the angle of attack of the airfoils.

16 airfoils of the airplane wings of OAF and ONERA types were considered. All the studied airfoils were asymmetrical, since they had some camber at different chord lengths. The geometries of the OAF095, OAF102, OAF117, OAF128 and OAF139 airfoils are similar to the geometries of the ONERA/Aerospatiale OAF095, …, ONERA/Aerospatiale OAF139 airfoils, respectively, except for the values of the leading edge radius and the trailing edge thickness, which vary in the ranges 0.001-0.0027% and 0.0002-0.0003%, respectively.

Let us compare the aerodynamic characteristics of the airfoils of the airplane wings by type based on the given calculated pressure values.

Airfoils of the OAF type have almost the same ratio of positive and negative pressures on the leading edge, upper and lower surfaces at zero angle of attack. A slight increase in negative pressure is observed on the surfaces of the OAF139 airfoil. During the climb, the highest ratio of positive and negative pressures (approximately 10 times) was determined for the OAF102 airfoil on the lower and upper surfaces from the leading edge, respectively. This leads to an increase in the drag of the airfoil when the airplane moves in the airspace. For the OAF139 airfoil, the climb in the air is more favorable, since the negative pressure near the leading edge is halved compared to the OAF102 airfoil. During the airplane descent, the minimum and maximum values of negative pressure near the leading edge are similarly determined for the OAF095 and OAF128 airfoils, respectively.

Since airfoils of the ONERA/Aerospatiale type had the slightly smaller leading edge radius, with a positive angle of attack, the negative pressure value increased, and with a negative angle of attack, the negative pressure value for the most airfoils decreased.

Analyzing the airfoils of the ONERA OA type, it was determined that the ONERA OA206 and ONERA OA209 airfoils are subjected to the greatest drag during horizontal flight and climb of the airplane, respectively. The ONERA OA213 airfoil is subjected to minimal drag under the considered flight conditions of the airplane. Minimum and maximum pressures occur in magnitude on the leading edge of the ONERA OA206 and ONERA OA212 airfoils at a negative angle of attack, respectively.

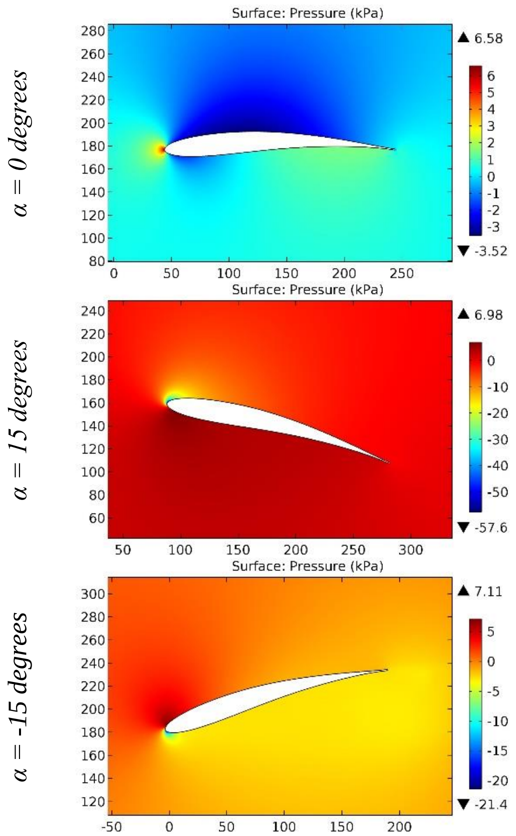

Figure 1. The pressure contours on the surfaces of the OAF095 airfoil.

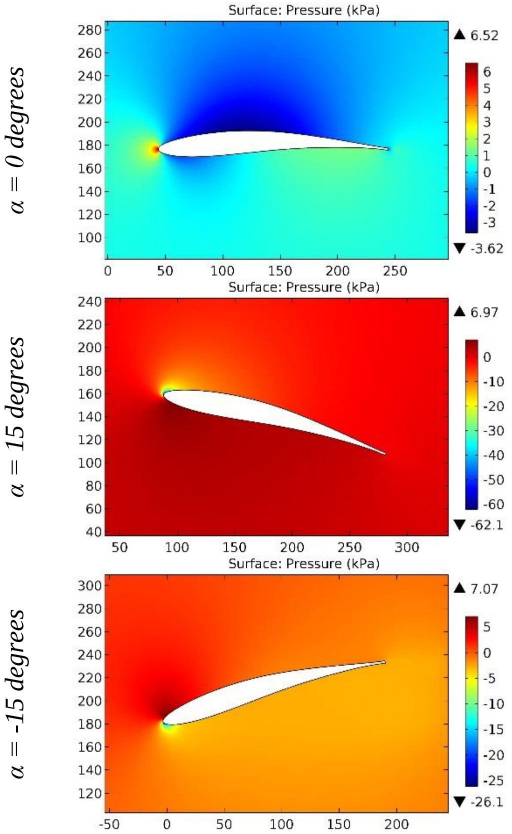

Figure 2. The pressure contours on the surfaces of the OAF102 airfoil.

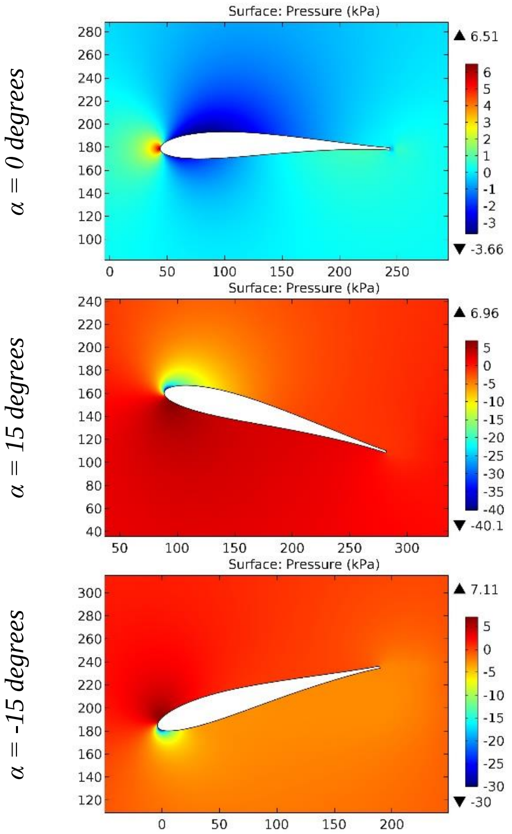

Figure 3. The pressure contours on the surfaces of the OAF117 airfoil.

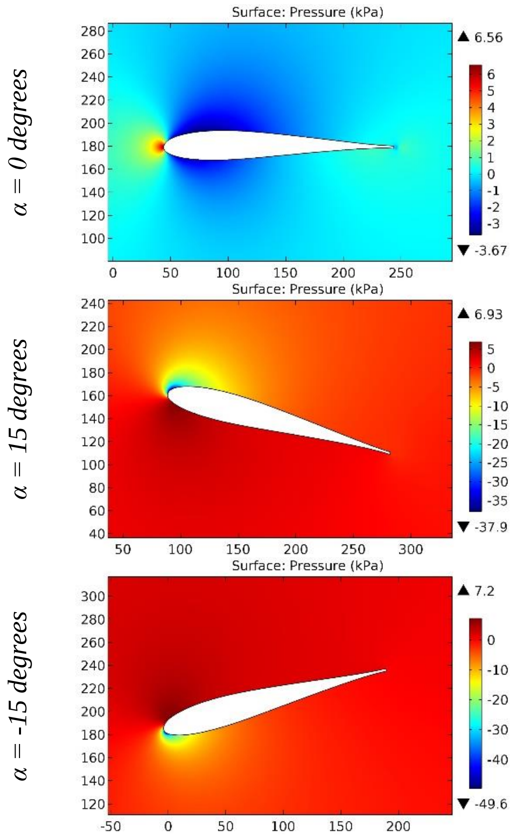

Figure 4. The pressure contours on the surfaces of the OAF128 airfoil.

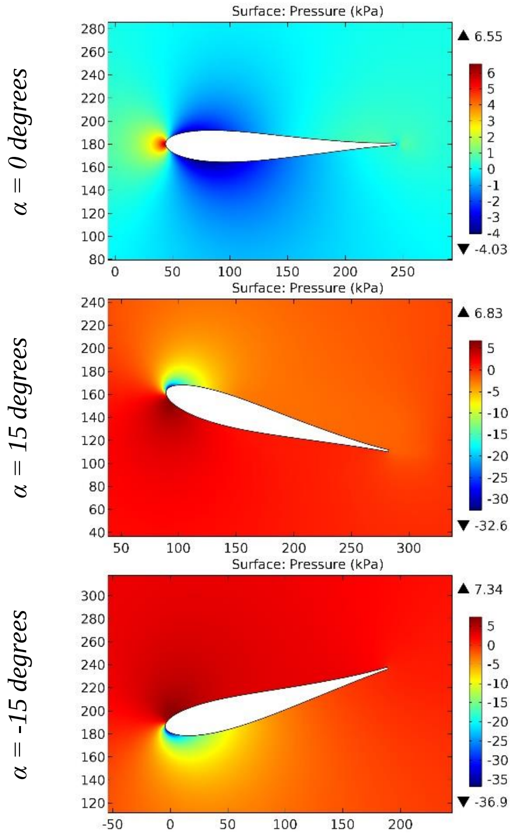

Figure 5. The pressure contours on the surfaces of the OAF139 airfoil.

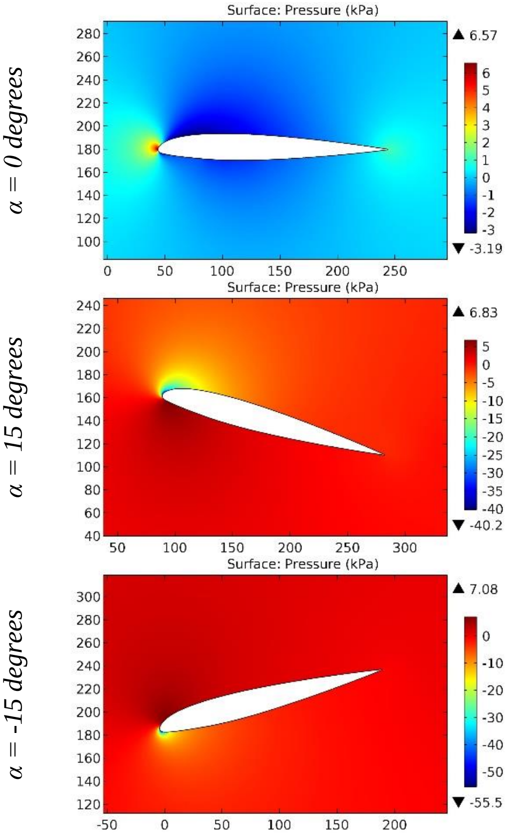

Figure 6. The pressure contours on the surfaces of the ONERA NACA CAMBRE airfoil.

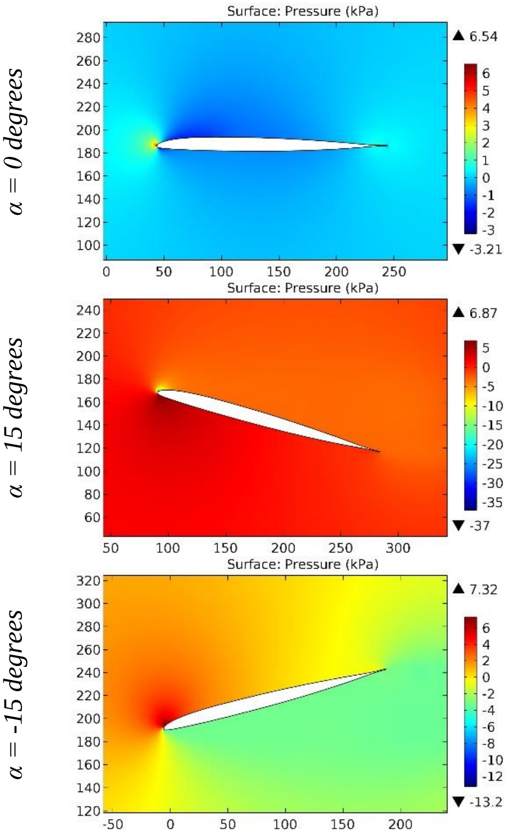

Figure 7. The pressure contours on the surfaces of the ONERA OA206 airfoil.

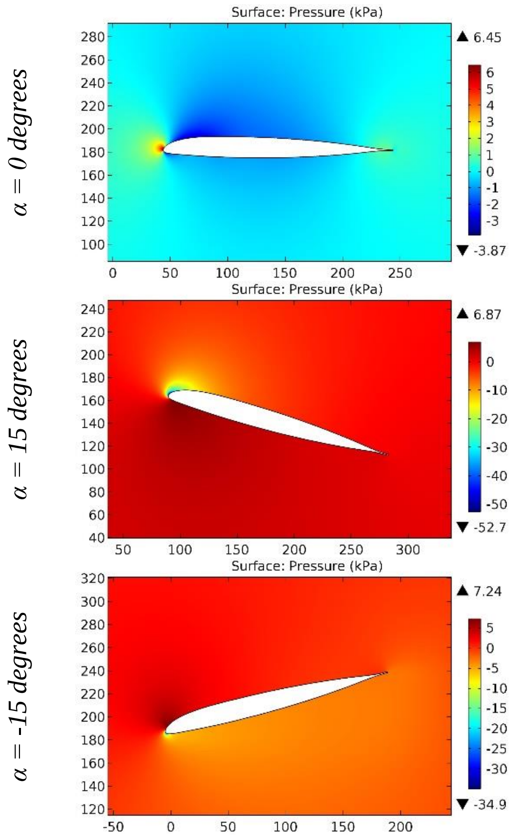

Figure 8. The pressure contours on the surfaces of the ONERA OA209 airfoil.

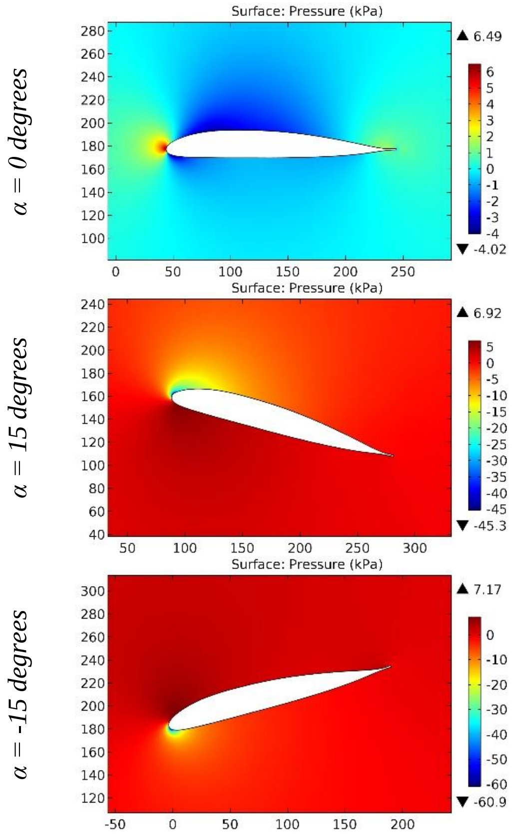

Figure 9. The pressure contours on the surfaces of the ONERA OA212 airfoil.

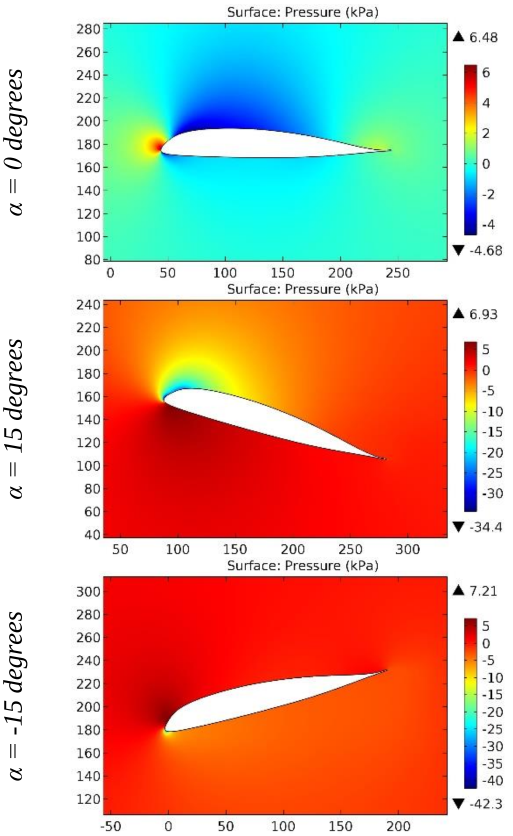

Figure 10. The pressure contours on the surfaces of the ONERA OA213 airfoil.

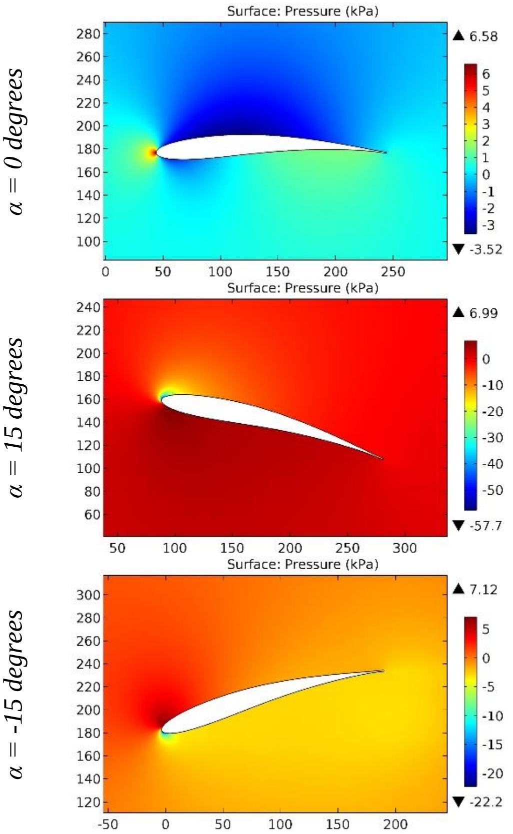

Figure 11. The pressure contours on the surfaces of the ONERA/Aerospatiale OAF095 airfoil.

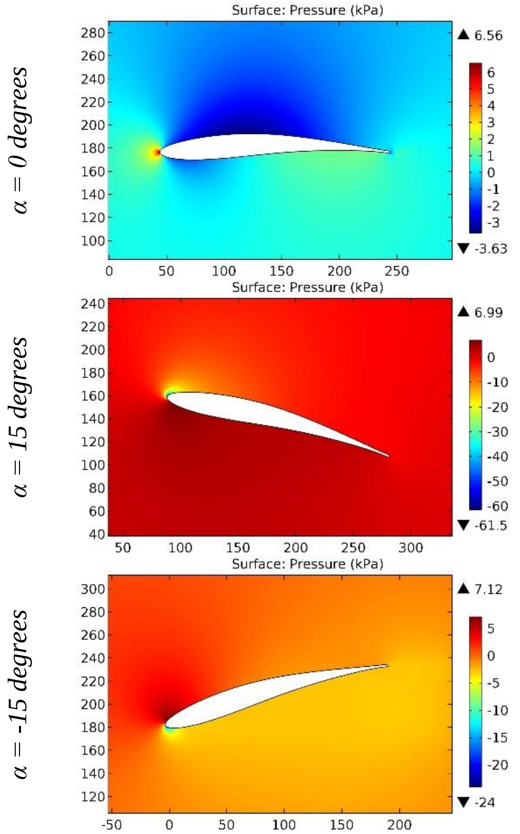

Figure 12. The pressure contours on the surfaces of the ONERA/Aerospatiale OAF102 airfoil.

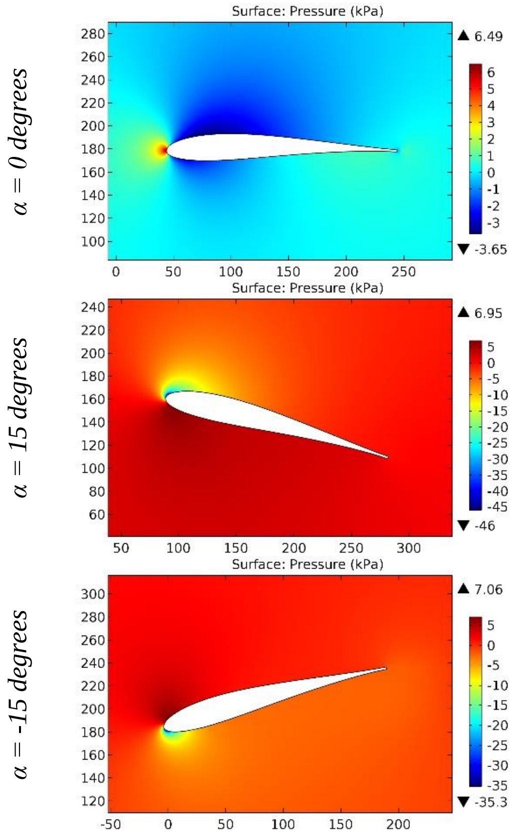

Figure 13. The pressure contours on the surfaces of the ONERA/Aerospatiale OAF117 airfoil.

Impact Factor:

ISRA (India)	= **6.317**	**SIS** (USA)	= **0.912**	**ICV** (Poland)	= **6.630**
ISI (Dubai, UAE)	= **1.582**	**РИНЦ** (Russia)	= **3.939**	**PIF** (India)	= **1.940**
GIF (Australia)	= **0.564**	**ESJI** (KZ)	= **8.771**	**IBI** (India)	= **4.260**
JIF	= **1.500**	**SJIF** (Morocco)	= **7.184**	**OAJI** (USA)	= **0.350**

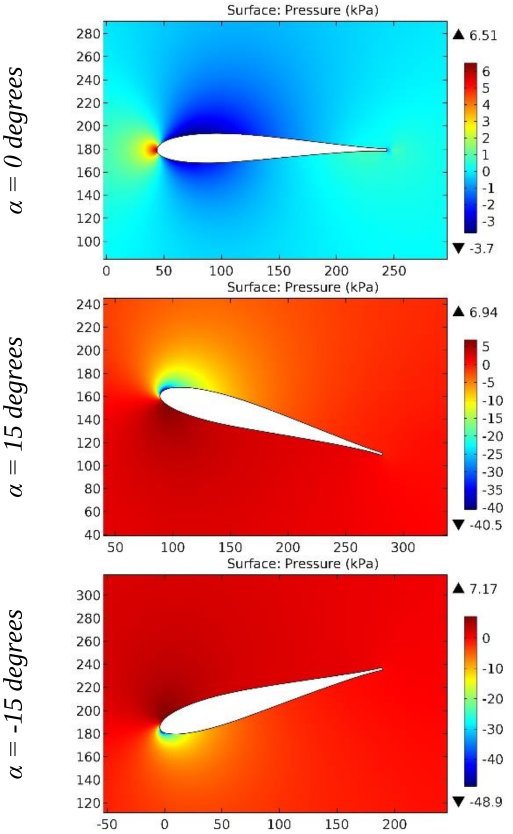

Figure 14. The pressure contours on the surfaces of the ONERA/Aerospatiale OAF128 airfoil.

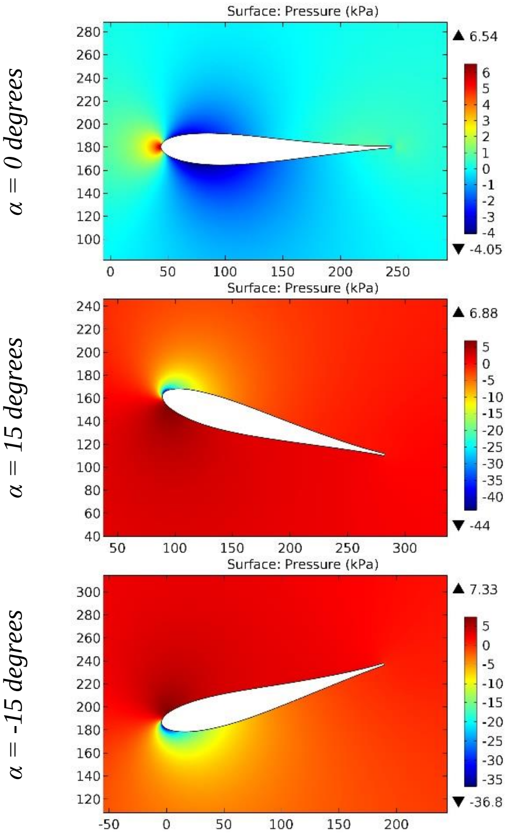

Figure 15. The pressure contours on the surfaces of the ONERA/Aerospatiale OAF139 airfoil.

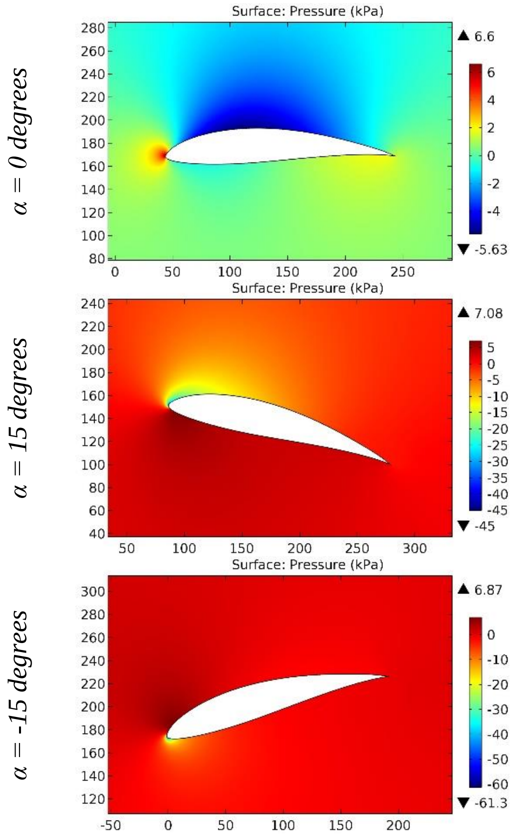

Figure 16. The pressure contours on the surfaces of the Ornithopter airfoil.

During the climb maneuver with the ONERA NACA CAMBRE airfoil, negative pressure is distributed over a larger area of the leading edge than during the descent maneuver. However, the maximum value of negative pressure is noted when the airplane descent.

The Ornithopter is subjected to the greatest drag in the leading edge area at a negative angle of attack of all the considered airfoils.

Conclusion

Based on the analysis of the results of computer calculation of the movement of airfoils in the airspace, the following conclusions can be drawn:

1. Negative pressure decreases with an increase in the leading edge radius of the airfoils of the same configuration. An increase in the leading edge radius by 0.0008% leads to a decrease in negative pressure by 14.5%, an increase in the leading edge radius by 0.0027% leads to a decrease in negative pressure by about 30%, etc.

2. The ONERA OA206 airfoil has the most optimal geometry, since in conditions of horizontal flight and maneuvers of the airplane, the wing experiences minimal loads, which are expressed by the action of negative pressure on the leading edge.

References:

1. Anderson, J. D. (2010). *Fundamentals of Aerodynamics.* McGraw-Hill, Fifth edition.
2. Shevell, R. S. (1989). *Fundamentals of Flight.* Prentice Hall, Second edition.
3. Houghton, E. L., & Carpenter, P. W. (2003). *Aerodynamics for Engineering Students*. Fifth edition, Elsevier.
4. Lan, E. C. T., & Roskam, J. (2003). *Airplane Aerodynamics and Performance.* DAR Corp.
5. Sadraey, M. (2009). *Aircraft Performance Analysis.* VDM Verlag Dr. Müller.
6. Anderson, J. D. (1999). *Aircraft Performance and Design*. McGraw-Hill.
7. Roskam, J. (2007). *Airplane Flight Dynamics and Automatic Flight Control*, Part I. DAR Corp.

8. Etkin, B., & Reid, L. D. (1996). *Dynamics of Flight, Stability and Control.* Third Edition, Wiley.
9. Stevens, B. L., & Lewis, F. L. (2003). *Aircraft Control and Simulation.* Second Edition, Wiley.
10. Chemezov, D., et al. (2021). Pressure distribution on the surfaces of the NACA 0012 airfoil under conditions of changing the angle of attack. *ISJ Theoretical & Applied Science, 09 (101)*, 601-606.
11. Chemezov, D., et al. (2021). Stressed state of surfaces of the NACA 0012 airfoil at high angles of attack. *ISJ Theoretical & Applied Science, 10 (102)*, 601-604.
12. Chemezov, D., et al. (2021). Reference data of pressure distribution on the surfaces of airfoils having the names beginning with the letter A (the first part). *ISJ Theoretical & Applied Science, 10 (102)*, 943-958.
13. Chemezov, D., et al. (2021). Reference data of pressure distribution on the surfaces of airfoils having the names beginning with the letter A (the second part). *ISJ Theoretical & Applied Science, 11 (103)*, 656-675.
14. Chemezov, D., et al. (2021). Reference data of pressure distribution on the surfaces of airfoils having the names beginning with the letter B. *ISJ Theoretical & Applied Science, 11 (103)*, 1001-1076.
15. Chemezov, D., et al. (2021). Reference data of pressure distribution on the surfaces of airfoils having the names beginning with the letter C. *ISJ Theoretical & Applied Science, 12 (104)*, 814-844.
16. Chemezov, D., et al. (2021). Reference data of pressure distribution on the surfaces of airfoils having the names beginning with the letter D. *ISJ Theoretical & Applied Science, 12 (104)*, 1244-1274.
17. Chemezov, D., et al. (2022). Reference data of pressure distribution on the surfaces of airfoils (hydrofoils) having the names beginning with the letter E (the first part). *ISJ Theoretical & Applied Science, 01 (105)*, 501-569.
18. Chemezov, D., et al. (2022). Reference data of pressure distribution on the surfaces of airfoils (hydrofoils) having the names beginning with the letter E (the second part). *ISJ Theoretical & Applied Science, 01 (105)*, 601-671.
19. Chemezov, D., et al. (2022). Reference data of pressure distribution on the surfaces of airfoils having the names beginning with the letter F. *ISJ Theoretical & Applied Science, 02 (106)*, 101-135.
20. Chemezov, D., et al. (2022). Reference data of pressure distribution on the surfaces of airfoils having the names beginning with the letter G (the first part). *ISJ Theoretical & Applied Science, 03 (107)*, 701-784.
21. Chemezov, D., et al. (2022). Reference data of pressure distribution on the surfaces of airfoils having the names beginning with the letter G (the second part). *ISJ Theoretical & Applied Science, 03 (107)*, 901-984.
22. Chemezov, D., et al. (2022). Reference data of pressure distribution on the surfaces of airfoils having the names beginning with the letter G (the third part). *ISJ Theoretical & Applied Science, 04 (108)*, 401-484.
23. Chemezov, D., et al. (2022). Reference data of pressure distribution on the surfaces of airfoils having the names beginning with the letter H (the first part). *ISJ Theoretical & Applied Science, 05 (109)*, 201-258.
24. Chemezov, D., et al. (2022). Reference data of pressure distribution on the surfaces of airfoils having the names beginning with the letter H (the second part). *ISJ Theoretical & Applied Science, 05 (109)*, 529-586.
25. Chemezov, D., et al. (2022). Reference data of pressure distribution on the surfaces of airfoils having the names beginning with the letter I. *ISJ Theoretical & Applied Science, 06 (110)*, 1-7.
26. Chemezov, D., et al. (2022). Reference data of pressure distribution on the surfaces of airfoils having the names beginning with the letter J. *ISJ Theoretical & Applied Science, 06 (110)*, 18-25.
27. Chemezov, D., et al. (2022). Reference data of pressure distribution on the surfaces of airfoils having the names beginning with the letter K. *ISJ Theoretical & Applied Science, 07 (111)*, 1-10.
28. Chemezov, D., et al. (2022). Reference data of pressure distribution on the surfaces of airfoils having the names beginning with the letter L. *ISJ Theoretical & Applied Science, 07 (111)*, 101-118.
29. Chemezov, D., et al. (2022). Reference data of pressure distribution on the surfaces of airfoils having the names beginning with the letter M. *ISJ Theoretical & Applied Science, 10 (114)*, 307-392.
30. Chemezov, D., et al. (2022). Reference data of pressure distribution on the surfaces of airfoils having the names beginning with the letter N (the first part). *ISJ Theoretical & Applied Science, 12 (116)*, 801-892.
31. Chemezov, D., et al. (2022). Reference data of pressure distribution on the surfaces of airfoils having the names beginning with the letter N (the second part). *ISJ Theoretical & Applied Science, 12 (116)*, 901-990.